

# Design, Modeling and Performance Investigation of GC

## PVGS

K.Rajambal, G.Renukadevi, N.K.Sakthivel

Department of Electrical Electronics Engg , Pondicherry Engineering College , Pondicherry ,India

\* E-mail of the corresponding author: [renunila\\_1977@yahoo.com](mailto:renunila_1977@yahoo.com)

### Abstract

This paper proposes a new topology for the power injection system that is based on the parallel association of two voltage source inverters: one is operated using a quasi-square voltage waveform strategy and the other operates with a PWM based strategy. The aim of this topology is that the quasi-square inverter injects the power from the photovoltaic generation system and the PWM inverter controls the current quality. The proposal optimizes the system design, permitting reduction of system losses and an increase of the energy injected into the grid.

**Keywords:** quasi square wave inverter, pulse width Modulation inverter, photo voltaic power system, modulation Index (M).

### 1. Introduction

Since the start of the industrial age more than 150Years ago, the world economy was running on fossil fuels, which were cheap as there was no cost associated with their Production, but only with their extraction and transportation. The negative effects on the environment became visible only in the last 30 years. Renewable energy resources will be increasingly important part of power generation in the new Millennium. Besides assisting in the reduction of the emission of greenhouse gases, they add the much needed flexibility to the energy resource mix by decreasing the dependence on Fossil fuels. Due to their modular characteristics, ease of the Installation and because they can be located closer to the user photovoltaic (PV) systems have great potential as distributed power source to the utilities. PV systems are installed on the roof of the residential buildings and connected directly to the grid.(called grid-tie or grid-connected ). A grid-tied PV system consists of two main stages a PV module and power injection System as shown in Figure. 1. In these PV systems , power Conditioning system (PCS) should have high efficiency and Low cost The power generated from the renewable energy systems are tied to the utility grid (Doumbia 2004) and (Jih-heng Lai 2003). In remote places where there is less/no feasibility of utility grids, renewable energy Systems provides electricity to the isolated region. These isolated renewable energy systems can be employed to power residential applications. For renewable energy sources, the output voltage and power typically depends on a variety of uncontrollable factors. for example: radiation intensity determines the obtainable voltage and power output of a solar panel, wind speed determines voltage and power of a wind electrical generator; and the output Voltage and power of a fuel cell changes with the operating temperature, fuel and air flow rates (Detrick 2005) to (DeSouza 2006). To obtain the required voltage output for varying input conditions, power conditioning Systems (PCS) are introduced as interfacing scheme between the PV panels and grid . The existing power conversion topologies used in power conditioning system consist of boost converter and a pulse width modulation inverter or a multi level inverter. The boost converter enhances the low voltage output from the renewable energy sources during low input conditions And the inverter converts the dc power into ac of required voltage and frequency. The two stage conversion system also increases the system cost and decreases the efficiency of the system. In this project, an inverter topology without the intermediate dc-dc converter has been presented. This scheme reduces the system losses and increases the efficiency and increase of the

energy injected into the grid. The proposed inverter is designed for a kW photovoltaic generation system. Photovoltaic generation scheme along with the inverter is simulated in MATLAB/Simulink. Simulation is carried out to study the power flow characteristics for varying solar intensities and modulation indices and the results are presented.

## 2. Description of the PvgS with QSWI-PWM Inverter

Fig.1 shows the inverter topology. This Photovoltaic Generation system presents a topology of the power injection system (PIS) that has the function of injecting the power produced by the photovoltaic cell groups, converting the energy from the original DC form to the final AC form with the desired electrical characteristics. The part of the PIS that carries out this conversion is the inverter (Carrasco 2006). Usually, Pulse width modulation (PWM) based inverters (Kwon 2006) or multilevel topology inverters are used (Gupta 2006). In this paper a new topology for the PIS is presented based on the parallel association of two voltage source inverters. (VSI): one is operated using a quasi-square voltage waveform strategy (quasi-square waveform inverter, QSWI). It can be operated with the operating frequency of grid frequency (50Hz) and the other operates with a PWM based strategy (high-switching-frequency inverter, HSFI). and this inverter can be operated as high switching frequency of 20kHz. The general purpose of the QSWI is to inject the power generated by the PVGS into the grid. In order to achieve this, controlling the fundamental component of the inverter and that of the HSFI is to be responsible for controlling the quality of the current injected into the grid. The mathematical modeling of the various system components are discussed below:

### (a) Modeling Of PV Cell

The characteristics of a solar cell relating the cells voltage to current are expressed by the equations, that are given below, The PV cell output current is given as,

$$I_{pv} = I_{ph} - I_0 \left[ \exp\left(\frac{q(V_{pv} + I_{pv}R_s)}{AKT}\right) - 1 \right] \quad \dots\dots (1)$$

The PV cell output voltage is given as,

$$V_{pv} = \frac{AKT}{q} \ln\left(\frac{I_{ph} - I_{pv} + I_0}{AKT}\right) - I_{pv}R_s \quad \dots\dots(2)$$

The light generated current is given as,

$$I_{ph} = [I_{scr} + K_i(T - 298)]\lambda / 100 \quad \dots\dots (3)$$

The saturation current is given as,

$$I_0 = I_{or} \left(\frac{T}{T_r}\right)^3 \exp\left[\frac{qE_{go}}{BK} \left(\frac{1}{T_r} - \frac{1}{T}\right)\right] \quad \dots\dots (4)$$

### (b) Power Injection System

A direct connection to the inverters without a previous DC/DC converter has been chosen. The upper inverter in the figure.1 (inverter 1) is the Quasi Square Wave Inverter and the lower inverter (inverter 2), is the High Switching Frequency Inverter. Both inverters share the same DC bus, which is connected to the PVGS. The capacitor between the PVGS and the PIS must absorb the active power fluctuations (that always exist in a single-phase system). Therefore it achieves constant power extracted from the PVGS, by keeping the DC voltage at the output terminal of the PVGS constant under these power fluctuations. The QSWI is responsible for injecting the energy produced by the PVGS. This inverter deals with high currents but at low switching frequency (50-60 Hz), resulting in lower losses than if the inverter is operated with a PWM technique. This inverter injects a current with a high total harmonic distortion (THD) into the grid. The PWMI is connected in parallel with the QSWI and working as a part of the PIS and its corrects the

current produced by the QSWI improving its THD. The PWMI (working as APF) not only can correct the QSWI current, but also correct the current demanded by a non-linear load connected to the same point of common coupling (PCC) than the PVGS. (Usually between 10 to 20 kHz).

**(C) Design of Inductance**

The QSWI inductance value (L1) must be selected to permit the injection of the maximum power That the PVGS can generate (which depends on the irradiance and temperature conditions). The power injected into the grid from the PVGS (neglecting the PIS losses),

$$P_s = V_s I_{s,1} = P_{PVGS} \dots\dots\dots (5)$$

As the current is in phase with the grid voltage. The RMS fundamental current component injected by the QSWI (I1) can be determined by ,

$$I_1 = \frac{\sqrt{V_1^2 - V_s^2}}{L_1 \omega} \dots\dots\dots (6)$$

From that two equations we get,

$$L_1 = \frac{V_s}{\omega P_{PVGS}} \sqrt{V_1^2 - V_s^2} \dots\dots\dots (7)$$

The inductance with proposed DC voltage is given by,

$$L_1 = \frac{V_s}{\omega P_{PVGS}} \sqrt{(0.9V_{dc} \cos \frac{\pi}{6})^2 - V_s^2} . \dots\dots\dots (8) \text{ and,}$$

$$L_2 = \frac{V_{dc} - \sqrt{2}V_s}{i_{2,slope}} \dots\dots\dots (9)$$

The coupled inductors enable the advantage of, output ripple current reduction due to AC magnetic field cancellation within the inductor core. Improved efficiency due to lower peak currents. Reduction in required output capacitance. Faster transient response due to the ability to use lower effective inductance values. Reduced overshoot or undershoot during load transients. Frequency range up to 2 MHz.

**3. Simulation Results**

The individual models of the PV array and inverters are simulated and their characteristics are studied. Then the models of PV array and inverters are integrated along with grid and simulation is carried out to study the power flow characteristics for varying solar intensities. The effect of modulation index is studied and the optimum modulation is identified for different solar intensities for maximizing the power output. The simulation results are discussed below,

**(a) Characteristics of the PV module.**

The model equations (1) - (4) of the PV cell detailed in section II (a) are used to obtain the I-V

characteristics of the PV module given in appendix. Figure.2 shows the I-V characteristics for varying solar intensities at constant temperature of 25°C. It observed that the current increases with increase in intensity thereby increasing the power output of the solar cell. It is observed that the PV array generates 550V Voltage and 8.8A current at the rated intensity of 100mW/cm<sup>2</sup> with 34 modules in series and 2 modules in parallel. Figure.3 shows that I-V characteristics for varying temperature at rated intensity of 100mW/cm<sup>2</sup>. It is observed that the current variation for marginal temperature variation from 25°C to 65°C. The output power versus power characteristics of the PV array for different intensity is shown in Figure.4 It is observed that the power increases with increasing voltage and reaches a maximum value and starts decreasing for any further increase in voltage. It is also seen that the output power increases with increasing intensity.

**(b) PIS results**

The quasi square wave inverter and pulse width modulation inverter are modeled in MATLAB-SIMULINK. The performance of the grid connected PIS which includes PWM and QSW Inverters are studied for different modulation indices. Figure.5 shows the firing pulses for Quasi Square Wave Inverter. A reference sine wave of 50Hz is compared with constant dc voltage to generate the firing pulse. The output voltage is varied by controlling the width of the pulse. In this switching scheme, the positive and negative half cycles are present for an interval less than the half the period of the output frequency. The QSWI is responsible for injecting the energy produced by the PVGS. The steady state voltage and current waveforms of the inverter are presented in Figures.6&7. It is seen that peak current of the QSWI is about 17 A without the controller. A reference sine wave of 50Hz is compared with triangular wave of 20 kHz to generate the firing pulse. The width of each pulse varies as a sine fashion. The frequency of the reference determines the output frequency of the inverter. The number of pulses in each half cycle depends on the carrier frequency. The output voltage is controlled by adjusting the modulation index. The PWMI is connected in parallel with the QSWI and working as a part of the PIS and its corrects the current produced by the QSWI improving its THD are seen from Figure.11. The main advantage of the proposed system is the inverter loss decrease, because the QSWI has low losses which are due principally to conduction. The switching losses are small because the switching frequency matches the grid frequency, near 50Hz. The conduction losses could be even further reduced if a low ON- voltage semiconductor is selected, since no high speed switching semiconductors are needed for this inverter. But also losses in the HSFI (principally due to the switching losses) decrease notably, because the current levels for this inverter are lower than those produced if it was working alone (without the QSWI cooperation). This can be observed in Figure.10. Where the maximum instantaneous current value is lower than 3 A, a value that is significantly lower than the maximum value of 15 A for the total injected current, Figure.11. If one assumes that the switching losses are proportional to the maximum instantaneous current value, these losses will be reduced to approximately 20%. Therefore the high switching semiconductors used in this inverter will have a current ratio of about five times lower than the semiconductor used in a conventional PWM inverter for the same task. The reduction in losses allows one to use a smaller aluminium radiator. Furthermore, the QSWI inductor can be built with a conventional core coil designed for a working frequency of 50 Hz (ferromagnetic core and conventional copper wire), and the HSFI inductor can be built with an air core coil with smaller section copper wire (usually special copper wires must be used due to the high switching frequency), because the RMS current value is smaller than if it operates alone.

**4. Control system**

The PIS control can be divided into the blocks shown in the schematic diagram of Figure. 12.

**(a) Maximum Power Point Tracking (MPPT) block:**

The objective of this block is to set and to maintain the PVGS at its maximum power point (MPP). When the PVGS is working at this point, one has that,

$$\frac{dP_{PVGS}}{dV_{PV}} = 0 \quad \dots\dots\dots (10)$$

The MPPT scheme is shown in Figure. 13. In the proposed system, this condition is achieved by

considering the power derivative as the error input of a proportional integral (PI) controller. In this way if the PI controller is well-designed, the power derivative will become zero in the steady state and the MPP will be tracked. A saturation function has been included to prevent the improper operation of the integral part of the controller during start-up transients. A low-pass filter is included to eliminate the components in the power derivative due to the switching frequency.

**(b) Reference Supply Current Generation Block**

This is the principal block of the proposed control system, because it guarantees that the current extracted from the PVGS is the desired one and so the MPP is tracked. The RMS value of the fundamental current component that must be injected into the grid is determined by neglecting the PIS losses:

$$I_{S,ref} = \frac{V_{PV} I_{PV,ref}}{V_S} \dots\dots\dots ( 11 )$$

This reference current value is tuned by the output of an additional PI whose input is the error between the reference current that must be extracted from the PVGS(determined by the MPPT block) and the actual one(measured from the system). The aim of this tuning is to compensate the system losses that have not been considered in (11).The RSCG block contains a synchronization module in fig.14. that generates two sinusoidal signals with unity RMS value, which are in phase (the first one) and in quadrature (the second one) with the fundamental grid voltage component, and an RMS grid voltage fundamental component calculation module .As a result the reference supply current is a sinusoidal wave in phase with the grid voltage, and its RMS value is equal to that given by (11).

**(c) Signal Generation for Inverter 1**

This block implements the collaboration between the two inverters and their principle of operation was described in above. Figures 15 and 16 shows the schematic diagram for each inverter. In Figure.15 the function block “Fcn” implements equation (11) , and the function block “Fcn1” is used to avoid values greater than 1 for the arc cosine function of this equation.

**(d) Switching Signal Generation for Inverter 2**

The QSWI is operated in a quasi-open-loop obtaining the value of β from the reference supply current (determined in part B), not its measured value. The HSF1 switching signals are generated based on the error existing between the reference supply current and the measured one, by using a hysteresis band that compares the error with zero for a fixed sample period (Figure.16).

**5. Controller results:**

The closed loop control systems are simulated with the parameters given in Appendix. The simulation results of the PVGS and Inverter are studied individually and the overall system performance for varying solar intensities and modulation indices are observed. From Figure.17 to 21 shows that the performance of the PVGS and the grid connected system results of the both inverter currents are simulated at rated intensity of 100mW/cm<sup>2</sup>. The main advantage of the proposed system is the inverter loss decrease, because the QSWI has low losses which are due principally to conduction. The switching losses are small because the switching frequency matches the grid frequency, near 50Hz. The conduction losses could be even further reduced if a low ON- voltage semiconductor is selected, since no high speed switching semiconductors are needed for this inverter. But also losses in the HSF1 (principally due to the switching losses) decrease notably, because the current levels for this inverter are lower than those produced if it was working alone (without the QSWI cooperation). This can be observed in Figure. 21. Where the maximum instantaneous current value is lower than 3 A, a value that is significantly lower than the maximum value of 15 A for the total injected current shown in Figure.22. If one assumes that the switching losses are proportional to the maximum instantaneous current value, these losses will be reduced to approximately 20%. Therefore the high switching semiconductors used in this inverter will have a current ratio of about five times lower than the semiconductor used in a conventional PWM inverter for the same task. The reduction in losses allows one to use a smaller aluminium radiator. Furthermore, the QSWI inductor can be built with a conventional core coil designed for a working frequency of 50 Hz (ferromagnetic core and conventional copper wire),

and the HSFI inductor can be built with an air core coil with smaller section copper wire (usually special copper wires must be used due to the high switching frequency), because the RMS current value is smaller than if it operates alone. The total inductor losses will be lower: (a) the electric losses in inductor of inverter 1 decrease because it has a lower resistance ( $R_1$ ) than if it had been built with air core coils (because far fewer turns of copper wire are needed). Ferromagnetic losses will be small since the operation frequency is 50 Hz. (b) the electric losses in inductor of inverter 2 decrease too, because the RMS of the current that flows through it ( $I_2$ ) is reduced by five times. Although the cost could seem to increase due to the more complex topology and control and to the higher number of semiconductors needed, other factors related to cost should be taken into account: decrease in losses and so decrease in the size of the aluminium radiator, possibility of using ferromagnetic core inductors for filtering the greater fraction of the current (these inductors are about 30% less expensive than air core inductors), possibility of using slower semiconductors (so cheaper devices) for the greater current fraction, and using lower rating high frequency semiconductors (because they operate with a lower current fraction).

### 6. Experimental results:

The prototype model of this scheme has been implemented in hardware. The prototype model has been tested with a laboratory Prototype (Figure.23) solar module (supplying 12 VDC) is connected to a four branches inverter (MOSFET-IRF840) and it can be connected into the load. The results are shown in Figure. 24 to 29. The proposed PIS behaves as in the simulation setup. The output voltage of the 15W PV module is found to vary from 15.07V to 18.09V over a day. The corresponding output voltages of the inverter are varying from 11.8V to 13.2V. The output voltage and current waveform are observed and presented. The hardware results are compared with the simulation results. It is found that the hardware result closely matches with the simulation results, thus validating the simulation model of the grid connected PVGS.

### 7. Conclusion

The power characteristics of the photovoltaic generation system is investigated for varying solar intensities. The power output of the photovoltaic module, the voltage and currents of the inverters and the power export to the grid are observed for different intensities. The effect of modulation index is studied and the optimum modulation is identified for every solar intensities for maximizing the power output. A closed loop control is designed to maximize the power output for varying intensities. The proposed system optimizes the system design, permitting the reduction of the system losses (conduction and switching losses, and Joule effect losses in inductors) and so increases the energy effectively injected into the grid. There will consequently be an increase in profit when selling this energy.

#### APPENDIX PV Generation System

Parameter	Value
Number of series connected cells	34
Number of parallel connected cells	2
Photovoltaic cell reference	SHELL BP150-P
MPP current (25°C, 100mW/cm <sup>2</sup> )	8.8A

MPP voltage (25°C, 100mW/cm <sup>2</sup> )	550V
Power rating at rated intensity of 100(mW/cm <sup>2</sup> )	3kW

Power Injection System

Filter inductance L1	50mh ×2
Filter inductance L2	25mH ×2
Switching frequency	20 kHz

REFERENCES:

- Doumbia.M.I.,Agbossou, K.;Bose, T.K.(2004), “Islanding protection evaluation of inverter-based grid-connected hybrid renewable energy system, Electrical and Computer Engineering”,1081-1084
- Jih-heng Lai (2003), “Power Electronics applications in renewable energy system”, Industrial Electronics Society, IECON.
- Detrick, A. Kimber, and L.Mitchell (2005), “Perfomance Evaluation Standards for Photovoltaic Modules and Systems,” proceedings of the 31th IEEE Photovoltaic Specialists Conference, Lake Buena Vista, FL.
- Armenta-Deu.C (.2003) “Prediction of battery behaviour in SAPV applications Renewable Energy” 28:1671-1684.
- K.C.A.deSouza,O.H.Goncalves,D.C.martins(2006). “study and optimization of two dc-dc power structures used in a grid- connected photovoltaic system”,power electronics specialists conference,PESC06,pp.1-5
- Carrasco. J.M, Franquelo, L.G Bialasiewicz. J.T, Galvan, E, Portillo-Guisado. R.C, Prats.M.A.M, Leon., J.I, Moreno-Alfonso.N (2006), “Power-Electronic Systems for the Grid Integration of Renewable Energy Sources: A Survey”. IEEE Transactions on Industrial Electronics, vol. 53, issue 4, pages:1002 - 1016.
- Weidong Xiao, Ozog, N.; Dunford.W.G (2007) “Topology Study of Photovoltaic Interface for Maximum Power Point Tracking”. IEEE Transactions on Industrial Electronics, vol 54, issue 3, pages 1696 – 1704.
- Kwon.J.-M, Nam.K.-H, Kwon.B.H (2006), “Photovoltaic Power Conditioning System with Line Connection”. IEEE Transactions on Industrial Electronics, vol. 53, issue 4, pages 1048- 1054.
- Gupta.A.K, Khambadkone.A.M (2006). “A Space Vector PWM Scheme for Multilevel Inverters Based on Two-Level Space Vector PWM”. IEEE Transactions on Industrial Electronics, vol. 53, issue 5, pages 1631 – 1639.
- Rico, Amparo,Cadaval, Enrique Romero; Montero, Maria Isabel Milanés (2007) “Power Injection Control System and Experimental Model based on Manufacturer Characteristic Curves for a Photovoltaic Generation System”. Compatibility in Power Electronics,CPE '07, pages 1 – 7. May 29 2007.

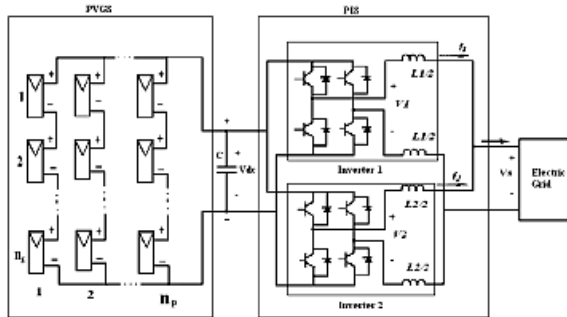


Figure.1. Power Conditioning System for a Grid connected Photovoltaic System

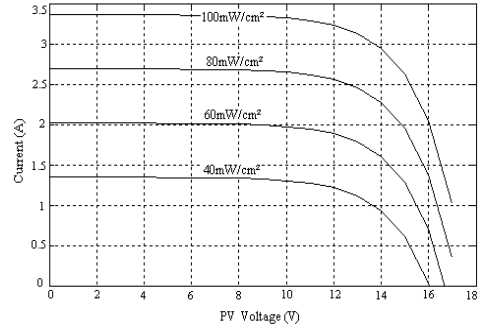


Figure.2 I-V characteristics of PV module for varying solar intensities at rated cell temperature

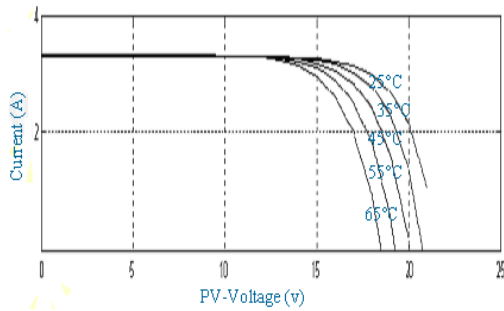


Figure.3 I-V characteristics of PV module for different cell temperature at rated intensity

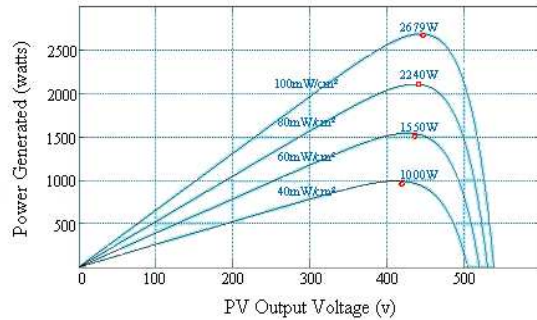


Figure. 4 Power characteristics for various solar intensities at rated cell temperature

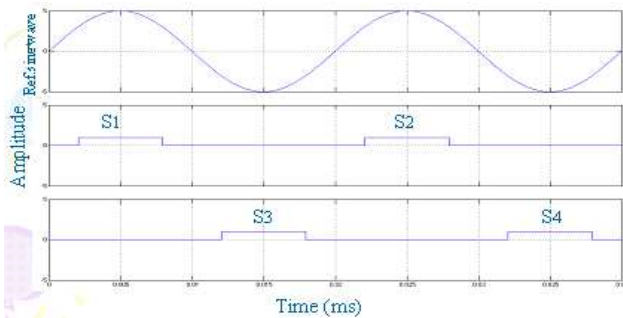


Figure.5. Firing pulse for QSWI

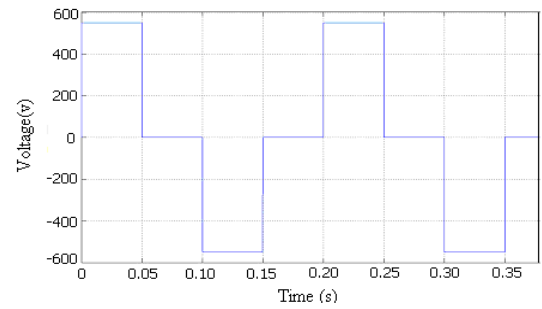


Figure.6. Quasi Square Wave Inverter Voltage

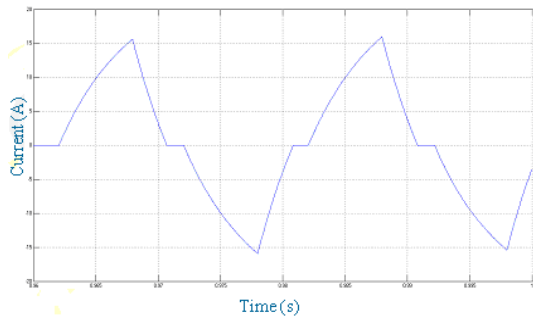


Figure.7. Quasi Square Wave Inverter Current

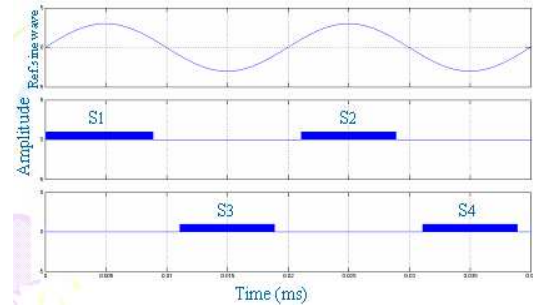


Figure.8. Firing pulse for PWM

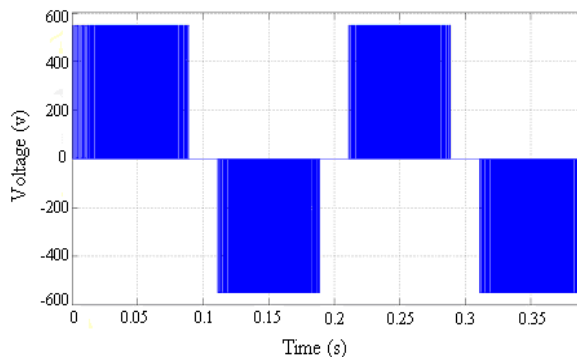


Figure.9. Pulse Width Modulation Inverter Voltage Current

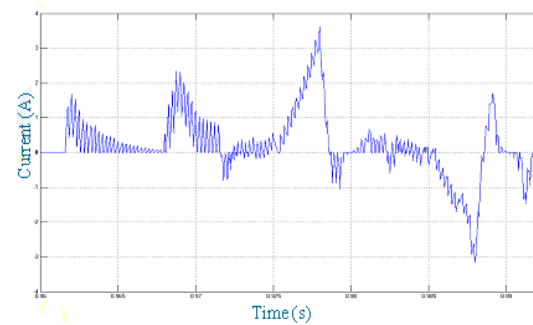


Figure.10. High Switching Frequency Inverter

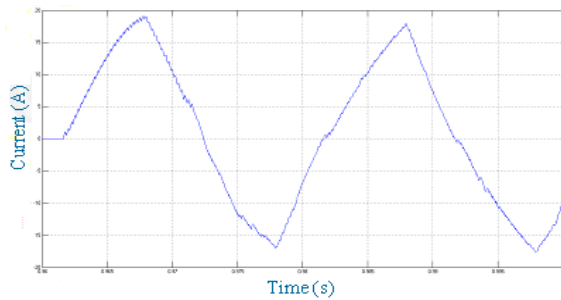


Figure.11. Current Injected into the grid

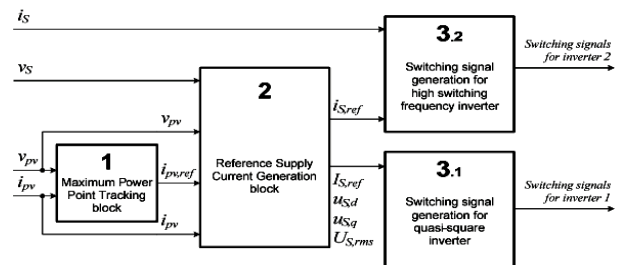


Figure.12 Maximum Power Point Tracking (MPPT)

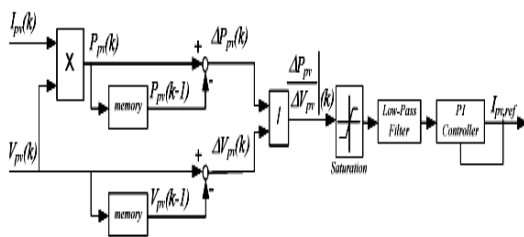


Figure.13 MPPT scheme

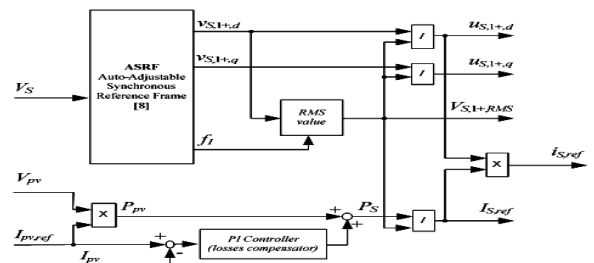


Figure.14.RSCG block contains a synchronization module

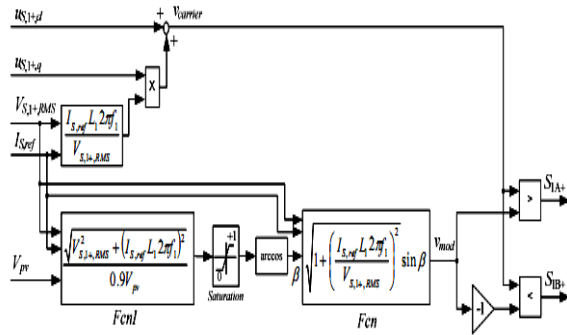


Figure.15. Inverter Switching

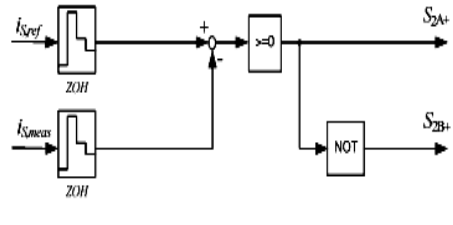


Figure.16. Inverter Switching

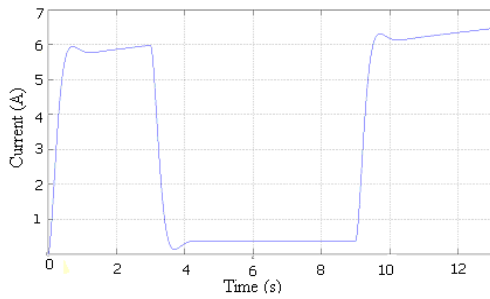


Figure.17 PVGS Current at 100mW/cm<sup>2</sup>

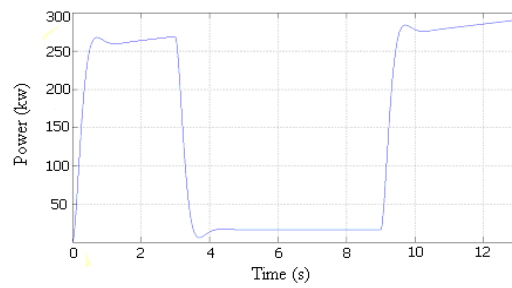


Figure.18 Power Extracted from the PVGS

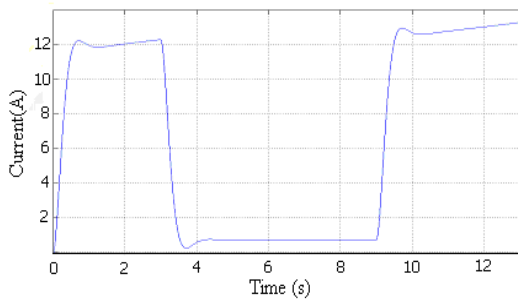


Figure.19 Supply reference current rms

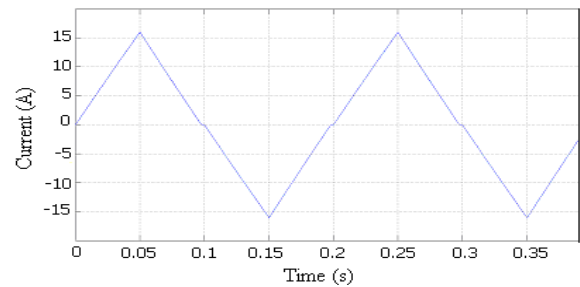


Figure.20. Quasi Square Wave Inverter Current

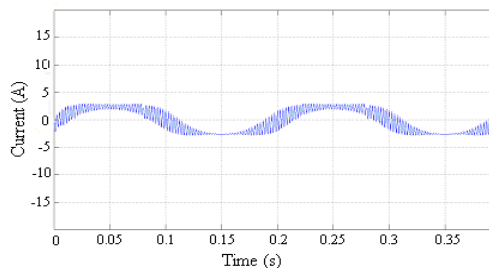


Figure.21. High Switching Frequency Inverter Current

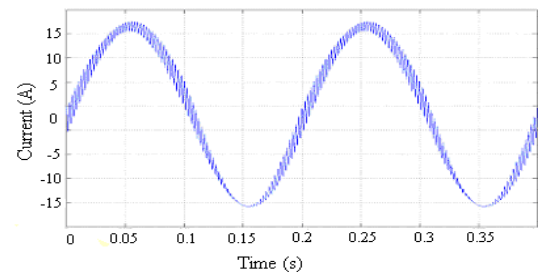


Figure.22. Current Injected into the grid

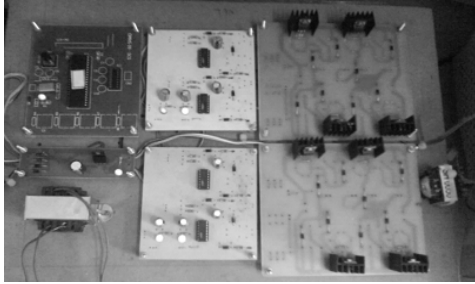


Figure.23. Hardware setup

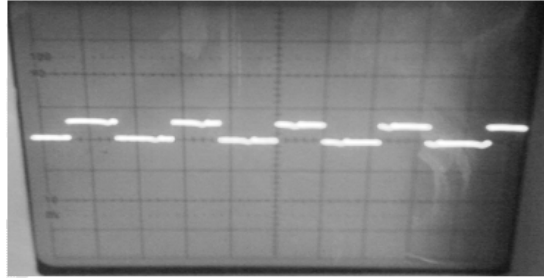


Figure.24. Firing pulse for QSWI

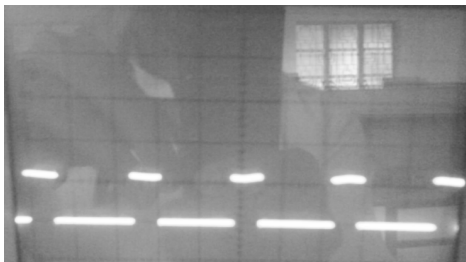


Figure.25. Firing pulse for PWMI

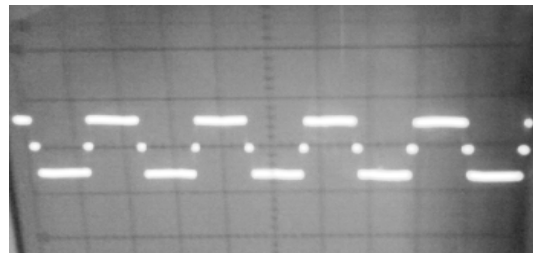


Figure.26. Quasi Square Wave Inverter Voltage

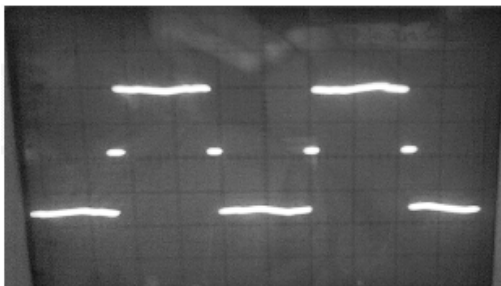


Figure.27. Pulse Width Modulation Inverter Voltage



Figure.28. High Switching Frequency Inverter Current

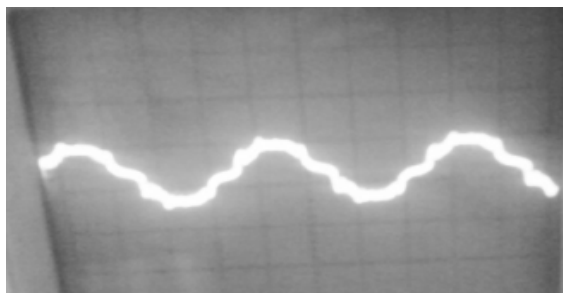


Fig.29. Load Voltage

Table 1

DC VOLTAGE	AC VOLTAGE	CURRENT	POWER
15	12.2	0.51	6.22
16	12.8	0.65	8.32
17	12.9	0.67	8.64
18	13.5	0.69	9.31

Table 2

TIME	DC VOLTAGE	AC VOLTAGE (Peak)	AC VOLTAGE (Rms)	CURRENT	POWER
9.30 am	15.07	16.68	11.8	0.49	5.78
10.30 am	15.19	17.53	12.4	0.54	6.69
11.30 am	16.16	18.10	12.8	0.62	7.93
12.30 pm	16.27	18.24	12.9	0.64	8.25
1.30 pm	18.09	18.66	13.2	0.66	8.71
2.30 pm	17.92	17.67	12.5	0.64	8.00
3.30 pm	15.08	16.68	11.8	0.60	7.08
4.30 pm	11.83	11.03	7.8	0.5	3.9

#### Bibliography of authors



K.Rajambal received her Bachelor of Engineering in Electrical & Electronics, Master of Engineering in power electronics and Ph.D in Wind Energy Systems in 1991, 1993 and 2005 respectively from Anna University, Chennai, India. She is working as a Associate professor in the Department of Electrical and Electronics in Pondicherry Engineering College, Pondicherry, India. Her area of interest includes in the fields of Wind Energy systems and Photovoltaic Cell, Power Converter such as DC-DC Converters, AC-AC Converters and Multilevel Inverters with soft switching PWM schemes and power electronics application towards power systems. She has published papers in national, international conferences and journals in the field of non renewable energy sources and power electronics.



G.Renukadevi received her Undergraduate Degree in Electrical Engineering from The Institution of Engineers, India in 2006 and Master of technology in Electrical Drives and Control from Pondicherry Engineering College, Pondicherry, India in 2009. Now pursuing Ph.D in Pondicherry Engineering College, Pondicherry, India. Her field of interest is power electronics, Drives and control, Modeling, AI techniques and control systems.

N.K.Sakthivel received Master of technology in Electrical Drives and Control in 2010 from Pondicherry Engineering College, Pondicherry, India in 2009. His field of interest is power electronics, renewable energy and control systems.

This academic article was published by The International Institute for Science, Technology and Education (IISTE). The IISTE is a pioneer in the Open Access Publishing service based in the U.S. and Europe. The aim of the institute is Accelerating Global Knowledge Sharing.

More information about the publisher can be found in the IISTE's homepage:

<http://www.iiste.org>

The IISTE is currently hosting more than 30 peer-reviewed academic journals and collaborating with academic institutions around the world. **Prospective authors of IISTE journals can find the submission instruction on the following page:**

<http://www.iiste.org/Journals/>

The IISTE editorial team promises to review and publish all the qualified submissions in a fast manner. All the journals articles are available online to the readers all over the world without financial, legal, or technical barriers other than those inseparable from gaining access to the internet itself. Printed version of the journals is also available upon request of readers and authors.

### **IISTE Knowledge Sharing Partners**

EBSCO, Index Copernicus, Ulrich's Periodicals Directory, JournalTOCS, PKP Open Archives Harvester, Bielefeld Academic Search Engine, Elektronische Zeitschriftenbibliothek EZB, Open J-Gate, OCLC WorldCat, Universe Digital Library, NewJour, Google Scholar

